

High-pressure Raman studies of polycrystalline BaTiO₃

Uma D. Venkateswaran

Department of Physics, Oakland University, Rochester, Michigan 48309

Vaman M. Naik

Department of Natural Sciences, University of Michigan-Dearborn, Dearborn, Michigan 48128

Ratna Naik

Department of Physics, Wayne State University, Detroit, Michigan 48202

(Received 30 June 1998)

We report Raman-scattering studies of polycrystalline BaTiO₃ under pressure up to 8.6 GPa. Our data show evidence for two structural phase transformations, one at around 2 GPa which corresponds to the previously reported tetragonal to cubic phase transition and a new one near 5 GPa. The persistence of strong Raman lines well beyond the tetragonal to cubic phase transition suggests the presence of significant disorder in the high-pressure cubic phase. In the case of polycrystalline samples, the disorder may arise not only from off-center positions of Ti atoms as was proposed earlier for single crystals but also due to grain boundaries and intergrain stresses. Raman spectra of other known phases of BaTiO₃ are also compared for possible contributions to the breakdown of Raman selection rules at high pressure. [S0163-1829(98)07645-0]

I. INTRODUCTION

Single crystalline BaTiO₃ is a well studied ferroelectric perovskite. It is known to undergo several phase transitions at ambient pressure as a function of temperature. Starting from low temperature, at ~ 193 K, BaTiO₃ transforms from a rhombohedral to an orthorhombic structure, which in turn changes to a tetragonal phase at ~ 280 K, and finally to a cubic phase at ~ 395 K.¹ A recently published pressure-temperature phase diagram² determined from dielectric constant measurements, confirms these phase changes in melt-grown single crystals of BaTiO₃. The ambient tetragonal phase is ferroelectric and the high-temperature cubic phase is paraelectric. The transition between the ferroelectric and the paraelectric phase has been studied as a function of temperature using both Raman and infrared spectroscopic measurements.³⁻⁵ The transition temperature has been shown to decrease when pressure is applied and the tetragonal to cubic transition occurs at ~ 2 GPa at room temperature.⁶ In the paraelectric cubic phase which exists for temperatures above 120 °C or pressures higher than 2 GPa, no Raman activity is expected since all atoms are located at sites with inversion symmetry. However, the presence of a Raman spectrum in the paraelectric phase has been reported at high temperatures up to 300 °C,⁷⁻⁹ and high pressures up to 3.5 GPa (Refs. 10,11) in single crystals of BaTiO₃. This result has been explained as due to the disorder in the position of the Ti atoms which breaks the Raman selection rules.

Recently, there is renewed interest in ferroelectric thin films for possible application as room-temperature pyroelectric infrared detectors and also in electronic and photonic devices.¹²⁻¹⁴ Polycrystalline films of ferroelectric barium strontium titanate (BST) grown by metallo-organic decomposition are being investigated for night vision applications.^{13,14} Vibrational spectroscopy such as infrared and Raman measurements are well suited for investigating

the relationship between ferroelectricity and lattice dynamics. The pressure behavior of the Raman spectrum of polycrystalline BaTiO₃ can provide a knowledge base for the interpretation of the spectra of polycrystalline BaTiO₃ and BST films which have built-in strain due to growth on lattice mismatched substrates such as platinum.¹⁵ In this paper, we report a Raman study of polycrystalline BaTiO₃ powder as a function of pressure and temperature. Our studies show that under the application of hydrostatic pressure, strong Raman modes persist up to 8.6 GPa, well beyond the ferroelectric to paraelectric phase transition. There is also evidence from our Raman data for two structural changes under pressure in polycrystalline BaTiO₃, one around 2 GPa and another near 5 GPa.

II. EXPERIMENTAL DETAILS

High-pressure Raman experiments at room temperature were carried out on a small piece ($\sim 100 \mu\text{m} \times 100 \mu\text{m} \times 100 \mu\text{m}$) of polycrystalline BaTiO₃ powder pressed between two diamond anvils. A gasketed Merrill-Bassett-type diamond-anvil cell was used in the back-scattering geometry. 4:1 methanol-ethanol mixture served as the hydrostatic pressure medium and the pressure was calibrated using the standard ruby fluorescence method. Pressure measurement with the ruby *R*-line shift is accurate to 3% or better and the alcohol mixture is known to be hydrostatic in the range of our pressure study at room temperature.¹⁶ Raman measurements at low temperatures were done using a closed cycle helium refrigerator (Janis Model CCS 150) and the temperature during Raman measurements was controlled to within $\pm 2^\circ$. Raman spectra were excited with less than 20 mW of 488.0 nm radiation from an argon ion laser focused to a spot size of $\sim 50 \mu\text{m}$ diameter. Scattered light was dispersed by a

double grating monochromator (Jobin Yvon Model HG2S) and detected by a cooled photomultiplier (Hamamatsu R943-02) and photon counting electronics. Entrance and exit slit widths were $300 \mu\text{m}$ which correspond to a spectral resolution better than 4 cm^{-1} . Data were obtained from two runs consisting of both the upward and downward cycles of pressure. Since there were no qualitative or quantitative differences between data from the two runs and also between the up and down pressure cycles, results are presented without any distinction. Generally, in high-pressure studies, it is not possible to obtain polarized spectra because (a) it is difficult to determine the orientation of the small piece of sample that is loaded into the pressure cell, and (b) of the depolarization of light in traversing the diamond windows. Thus, all spectra reported in this study on polycrystalline BaTiO_3 are unpolarized.

III. RESULTS AND DISCUSSION

Both in the paraelectric and ferroelectric phase, BaTiO_3 has one molecule (5 atoms) per unit cell. Therefore, there are twelve ($3 \times 5 - 3$) long wavelength optical modes. The paraelectric phase which exists above 400 K, has cubic (O_h or $Pm3m$) symmetry. The optical modes in this phase transform according to triply degenerate irreducible representations $3F_{1u} + F_{2u}$ of the O_h point group. The F_{2u} mode is silent and the F_{1u} modes are only infrared active and so there is no Raman activity in the paraelectric phase with perfect cubic symmetry. In the ferroelectric phase with tetragonal (C_{4v}^1 or $P4mm$) symmetry, each of the F_{1u} modes splits into a doubly degenerate E mode and a nondegenerate A_1 mode, and the F_{2u} mode splits into E and B_1 modes. Thus, $\Gamma_{C_{4v}^1}^{\text{optic}} = 3(A_1 + E) + E + B_1$. All the A_1 and E modes are both Raman and infrared active and the B_1 mode is only Raman active. The presence of long-range electrostatic forces further splits each of the A_1 and E modes into transverse and longitudinal optical (TO and LO) modes. The assignments, both symmetry and nature (first or second order), of the observed Raman and infrared frequencies have remained somewhat controversial in the early work.^{5,17} However, detailed Raman¹⁸⁻²¹ and infrared⁵ studies on single crystalline BaTiO_3 have discussed the assignments of the different mode frequencies. A compilation of the optical phonon frequencies and their symmetry in tetragonal BaTiO_3 are given in Table I.

Figure 1 shows the room temperature Raman spectra of BaTiO_3 polycrystalline powder for several pressures between atmospheric pressure and 3.5 GPa. The dominant features in the 1 bar spectrum (bottom trace in Fig. 1), taken outside the diamond cell, are a broad peak centered near 265 cm^{-1} [$A_1(\text{TO})$], a sharp peak at 315 cm^{-1} [B_1 , $E(\text{TO}+\text{LO})$], an asymmetric and broad peak near 520 cm^{-1} [A_1 , $E(\text{TO})$], and a broad, weak peak at around 720 cm^{-1} [A_1 , $E(\text{LO})$], where the phonon assignment is given inside square brackets. The observed Raman peaks have been assigned to more than one phonon mode since the frequencies of a few A_1 and E modes are very close (see Table I) and also the different orientations of the crystallites in a polycrystalline sample does not permit polarization selection between the A_1 and E modes. The ob-

TABLE I. Optical phonon frequencies (ω) and their mode symmetry assignments in tetragonal BaTiO_3 .

$\omega \text{ (cm}^{-1}\text{)}$	Symmetry	Reference
36	$E(\text{TO})$	20
170	$A_1(\text{TO})$	18,21
180	$E(\text{TO}), E(\text{LO})$	20
185	$A_1(\text{LO})$	18,21
270	$A_1(\text{TO})$	18,21
305	$E(\text{TO}+\text{LO})$	20
305	B_1	20
463	$E(\text{LO})$	20
475	$A_1(\text{LO})$	18,21
486	$E(\text{TO})$	20
518	$E(\text{TO})$	20
520	$A_1(\text{TO})$	18,21
715	$E(\text{LO})$	20
720	$A_1(\text{LO})$	18,21

served spectrum at 1 bar agrees well with the powder Raman spectrum reported by Burns and Scott²¹ and also with those reported for ceramic and polycrystalline films grown by metal-organic chemical vapor deposition.²² It compares well with the single crystal data^{10,11} except for a dip²³ near 186 cm^{-1} which has been understood as an interference due to the anharmonic coupling between the three $A_1(\text{TO})$ phonons. As the applied pressure is increased, the $A_1(\text{TO})$

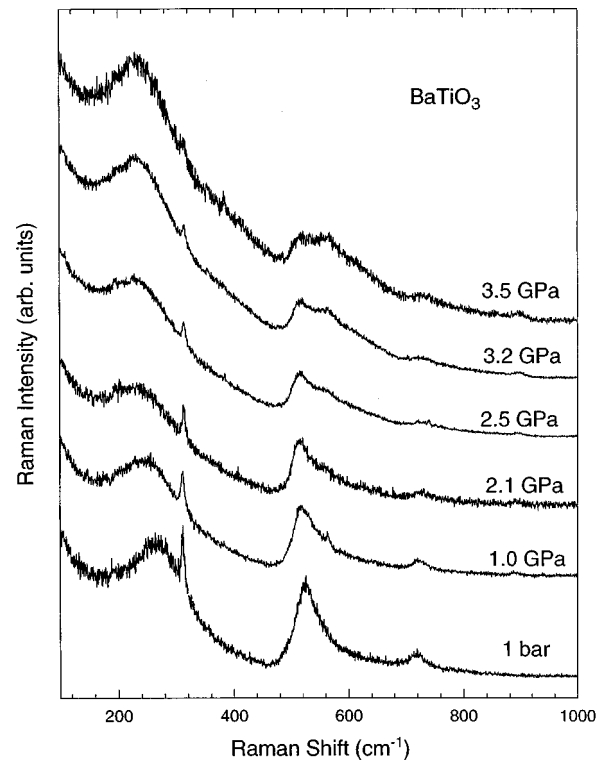


FIG. 1. Unpolarized Raman spectra of polycrystalline BaTiO_3 for several pressures between atmospheric pressure and 3.5 GPa recorded at room temperature. Notice the gradual weakening and disappearance of the sharp peak at 305 cm^{-1} and the line shape changes in the region between $500\text{--}600 \text{ cm}^{-1}$.

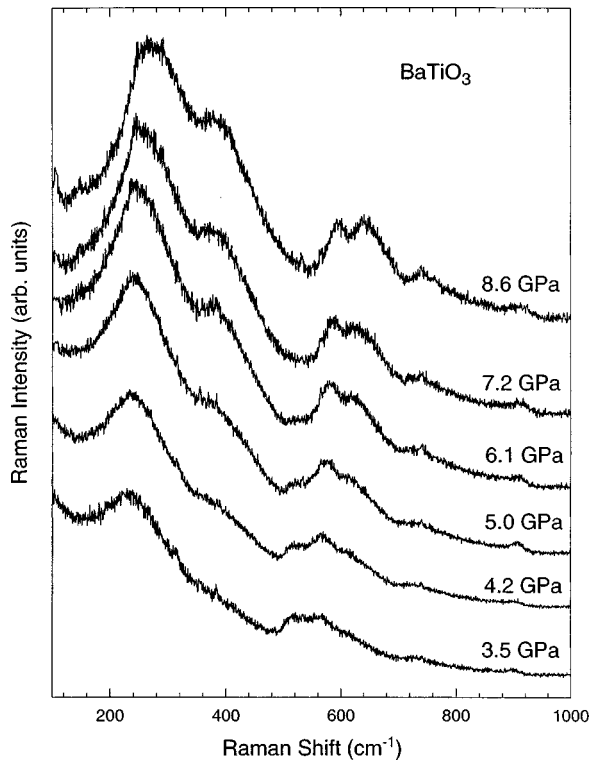


FIG. 2. Unpolarized Raman spectra of polycrystalline BaTiO_3 recorded at room temperature and elevated pressure between 3.5 and 8.6 GPa. Noticeable changes are apparent in the spectral line shape between 180–450 and 480–680 cm^{-1} as the applied pressure increases.

phonon peak at 265 cm^{-1} shifts to lower frequency up to 2.5 GPa, beyond which it shifts to higher frequency. The sharp peak at 310 cm^{-1} remains at the same frequency position but gradually weakens and disappears above 3.5 GPa. In the 500–600 cm^{-1} region, there is a significant change in the line shape. The $A_1, E(\text{TO})$ peak shows a second peak on the high-frequency asymmetric tail for pressures above 1 GPa which becomes more distinct as a separate peak between 2.5 and 3.5 GPa. At 3.5 GPa, two Raman peaks of almost equal intensity are clearly discernable. The LO phonon at 720 cm^{-1} becomes progressively weak and broad under pressure and exhibits no significant pressure shift in its frequency position. A weak peak seen near 883 cm^{-1} in all high-pressure spectra is from the pressure medium. Its frequency position and pressure shift (4.3 $\text{cm}^{-1}/\text{GPa}$) correspond to the C-C stretching mode of ethanol.²⁴

Figure 2 shows the Raman spectra observed at pressures higher than those shown in Fig. 1. The spectrum at 3.5 GPa is repeated in Fig. 2 for continuity. It is interesting to note that strong Raman spectra persist all the way up to 8.6 GPa, well beyond the transition to the paraelectric phase. In previous high-pressure studies on single crystalline BaTiO_3 ,^{10,11} the Raman modes of the tetragonal phase were found to weaken near 1.9 GPa, and only a weak spectrum with broad features has been observed in the paraelectric phase between 2 and 3.5 GPa. This suggests that the disorder is more pronounced in the polycrystalline material. Significant changes in the Raman spectra seen above 3.5 GPa are (a) increase in the intensity of the lowest energy phonon (near 250 cm^{-1})

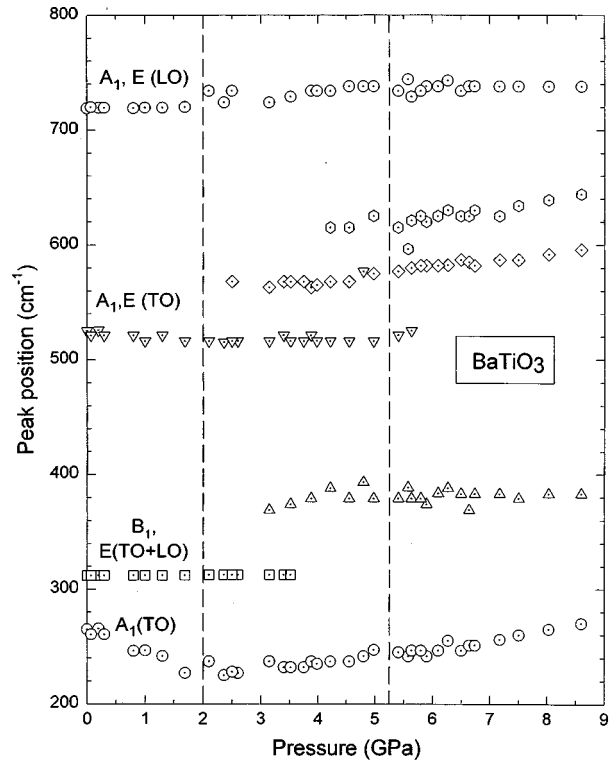


FIG. 3. Frequency of the Raman peaks observed in polycrystalline BaTiO_3 plotted as a function of pressure. Splitting or disappearance of modes and discontinuities in the slopes indicate structural reordering in the sample.

as pressure increases, (b) the development of a shoulder near 400 cm^{-1} which grows into a distinct peak with substantial intensity above 6 GPa, (c) the line shape changes in the region of 480–680 cm^{-1} : between 4 and 6 GPa, three peaks at 520, 560, and 620 cm^{-1} can be seen, the lowest frequency peak which was dominant below 3 GPa, disappears above 6 GPa, and (d) the apparent sharpening of the Raman peak near 720 cm^{-1} . We believe that the splitting and disappearance of Raman peaks resulting in the observed line shape changes are indicative of some structural reordering taking place near 5 GPa.

The frequency positions of all the observed Raman peaks are plotted as a function of pressure in Fig. 3. The error in determining the frequency position is not more than the size of the symbols in this plot. The frequency of the $A_1(\text{TO})$ phonon decreases at a rate of $\sim 20.8 \text{ cm}^{-1}/\text{GPa}$ in the pressure range of 0–2 GPa, increases by $\sim 6.6 \text{ cm}^{-1}/\text{GPa}$ between 2.5–5.2 GPa, and then increases at a rate of $13.8 \text{ cm}^{-1}/\text{GPa}$ between 5.5 and 8.6 GPa. The sharp $B_1, E(\text{TO}+\text{LO})$ mode (at 315 cm^{-1} at 1 bar), and the $A_1, E(\text{TO})$ mode (at 520 cm^{-1}) do not show any significant pressure-induced frequency shift. The $A_1, E(\text{LO})$ mode frequency (720 cm^{-1}) is more or less pressure insensitive in the 0–2 and 5–9 GPa ranges and shows a shift of about 4.5 $\text{cm}^{-1}/\text{GPa}$ between 2 and 5 GPa. The softening of the $A_1(\text{TO})$ phonon, the gradual weakening and disappearance of the sharp peak at 315 cm^{-1} , the decrease in the intensity of the 520 and 720 cm^{-1} peaks, and their negligible pressure shifts are consistent with the characteristics

reported for the ferroelectric to paraelectric phase transition in single crystals of BaTiO_3 .¹⁰ The line shape changes observed near $350\text{--}600\text{ cm}^{-1}$ between 3.5 and 9 GPa (see Fig. 2) correspond well with discontinuities in the slopes of the phonon frequency shifts shown in Fig. 3. Although the frequency positions plotted in Fig. 3 are as read from the spectra, we have verified their values by fitting a sum of several Lorentzians and a baseline to the normalized Raman spectra at four representative pressures, viz., 1 bar, 3.5 GPa, 5 GPa, and 8.6 GPa. The best fit curves contain five, six, seven, and six Lorentzians, respectively, i.e., the number of fitted Lorentzians is one more than the number of peaks plotted in Fig. 3 at these pressures. This is because a broad peak with low intensity was needed around 600 cm^{-1} in all the spectra to arrive at the best fit. The qualitative trends described earlier in regard to Figs. 1–3, were confirmed from the fitting parameters (peak position, width, and amplitude).

Thus, from the high-pressure Raman measurements on polycrystalline BaTiO_3 presented in Figs. 1–3, we infer that there are two structural rearrangements, one between 2 and 2.7 GPa which corresponds to the well-studied ferroelectric to paraelectric transition and a second one near 5 GPa which has not been reported for BaTiO_3 . The presence of Raman modes of high intensity in the paraelectric phase implies that this phase does not have perfect cubic symmetry but has some disorder which breaks the symmetry and permits Raman activity. This disordered cubic phase exists between 3 and 5 GPa, and undergoes another structural reordering around 5 GPa, evidenced by the lineshape changes observed in the Raman data.

Unlike x-ray diffraction, Raman spectroscopy does not provide a direct structural determination; but it is more sensitive to instantaneous changes in atomic positions. In the case of single crystalline BaTiO_3 , disorder in the paraelectric cubic phase has been noted in diffuse x-ray scattering studies²⁵ and also in Raman studies at high temperature^{7–9} and high pressure up to 3.5 GPa.¹¹ Based on the order-disorder model for the ferroelectric to paraelectric transition, the disorder in the paraelectric phase is associated with the position of the Ti atoms. Instead of occupying the body center positions as in a perfect cubic perovskite structure, the Ti atoms are, on the average, thought to be displaced along the cube diagonals²⁵ causing the disorder. In polycrystalline material there are additional mechanisms such as grain boundaries and intergrain stresses that could break Raman selection rules. Furthermore, at elevated pressures, it is possible to produce distortions in the cubic phase to other known phases of BaTiO_3 . High-pressure x-ray studies on polycrystalline BaTiO_3 will be needed to determine the disorder in the cubic phase as well as the structure of the phase above 5 GPa. In the absence of such a study, it is worth looking at the Raman spectra of other known phases of BaTiO_3 . Hexagonal (*h*) BaTiO_3 is a known polymorphic form and its Raman spectrum has been studied under pressure by Akishige *et al.*²⁶ The frequencies of all the phonons in the *h* phase are lower than 220 cm^{-1} at atmospheric pressure and they shift to higher frequencies at a rate ranging from 2 to $4\text{ cm}^{-1}/\text{GPa}$.²⁶ Two of the Raman modes at 175 and 220 cm^{-1} may contribute to the Raman spectrum observed in polycrystalline BaTiO_3 above 4 GPa (see Fig. 2). The other well known low-temperature phases are orthorhombic

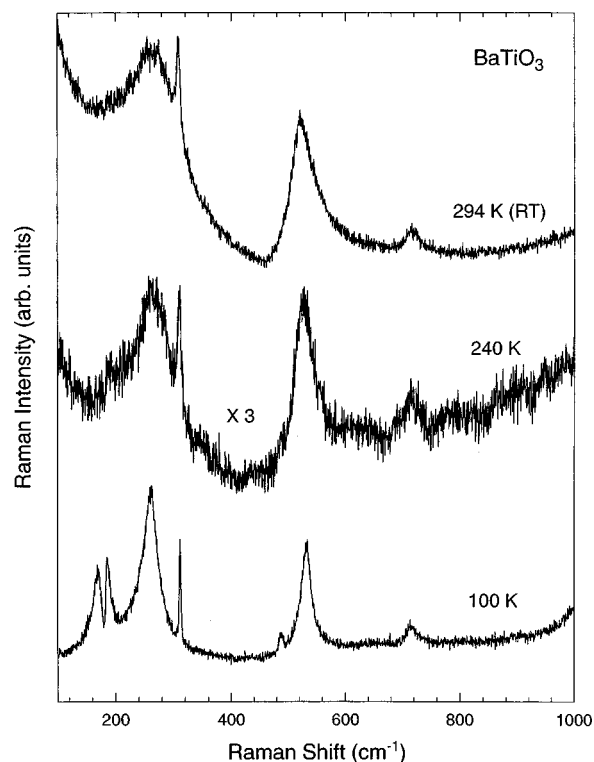


FIG. 4. Temperature dependence of the Raman spectra of polycrystalline BaTiO_3 . Spectra at 100, 240, and 294 K correspond to rhombohedral, orthorhombic, and tetragonal phases, respectively.

(*o*) and rhombohedral (*r*) as mentioned in the Introduction. The Raman spectra of polycrystalline BaTiO_3 recorded at various temperatures are shown in Fig. 4. Since the *o* phase exists between 290 and 193 K, the spectrum at 240 K corresponds to this phase. This spectrum is very similar to that of the tetragonal phase but with much weaker intensity. A weak peak around 600 cm^{-1} is a notable change. The *r*-phase spectrum at 100 K, regains intensity and exhibits splitting and sharpening of Raman modes. Although the application of high pressure and low temperature decreases the lattice constant, pressure effects are solely due to volume changes whereas phonon population changes also contribute to temperature effects. Therefore, a direct comparison of low temperature data with those at elevated pressure is not straightforward. Finally, we note that the observed changes in the Raman spectra at elevated pressures need not be due to contributions from *r*, *o*, or *h* phases but may be due to structural distortions caused by the movement of the atoms from regular lattice sites to interstitial positions by the application of pressure.

In summary, a high-pressure Raman study of polycrystalline BaTiO_3 reveals strong Raman modes up to 8.6 GPa well beyond the tetragonal to cubic phase transition. Since no Raman activity is expected in the cubic phase which exists above 2 GPa, the observation of the Raman spectrum at high pressures is attributed to the presence of disorder. The disorder is more pronounced in polycrystalline BaTiO_3 than previously reported in single crystals, most likely due to the presence of grain boundaries and intergrain stresses or increased disorder in atomic positions under pressure. There is no pressure-induced amorphization since the observed Raman spectra are as sharp as that at 1 bar. The evolution of the Raman spectrum under pressure indicates that there are at

least two structural phase changes. The first one, occurring near 2 GPa, corresponds to the transition from a ferroelectric tetragonal to a paraelectric disordered cubic phase. The second transition occurs near 5 GPa. Further x-ray studies at elevated pressures are needed to determine the structure of the high-pressure phase.

ACKNOWLEDGMENTS

The authors acknowledge the help of Christopher Flattery in fitting Lorentzian profiles to the data and Dr. Joseph Mantese of General Motors R and D Center for initiating this work.

-
- ¹F. Jona and G. Shirane, *Ferroelectric Crystals* (Pergamon, London, 1962).
- ²T. Ishidate, S. Abe, H. Takahashi, and N. Mori, *Phys. Rev. Lett.* **78**, 2397 (1997).
- ³A. Chaves, R. S. Katiyar, and S. P. S. Porto, *Phys. Rev. B* **10**, 3522 (1974).
- ⁴A. Scalabrin, A. S. Chaves, D. S. Shim, and S. P. S. Porto, *Phys. Status Solidi* **79**, 731 (1977).
- ⁵J. A. Sanjurjo, R. S. Katiyar, and S. P. S. Porto, *Phys. Rev. B* **22**, 2396 (1980).
- ⁶L-G. Liu and W. A. Bassett, *Elements, Oxides, and Silicates* (Oxford University Press, New York, 1986).
- ⁷M. P. Fontana and M. Lambert, *Solid State Commun.* **10**, 1 (1972).
- ⁸G. A. Barbosa, A. Chaves, and S. P. S. Porto, *Solid State Commun.* **11**, 1053 (1972).
- ⁹A. M. Quittet and M. Lambert, *Solid State Commun.* **12**, 1053 (1973).
- ¹⁰A. Jayaraman, J. P. Remeika, and R. S. Katiyar, in *Defect Properties and Processing of High Technology Nonmetallic Metals*, edited by J. H. Crawford, Jr., Y. Chen, and W. A. Sibley, MRS Symposia Proceedings No. 22 (Materials Research Society, Pittsburgh, 1984), p. 165.
- ¹¹A. K. Sood, N. Chandrabhas, D. V. S. Muthu, and A. Jayaraman, *Phys. Rev. B* **51**, 8892 (1995).
- ¹²N. W. Schubring, J. V. Mantese, A. L. Micheli, A. B. Catalan, and R. J. Lopez, *Phys. Rev. Lett.* **68**, 1778 (1992).
- ¹³M. S. Mohammed, R. Naik, J. V. Mantese, N. W. Schubring, A. L. Micheli, and A. B. Catalan, *J. Mater. Res.* **11**, 2588 (1996).
- ¹⁴M. S. Mohammed, G. W. Auner, R. Naik, J. V. Mantese, N. W. Schubring, A. L. Micheli, and A. B. Catalan, *J. Appl. Phys.* **84**, 3322 (1998).
- ¹⁵V. M. Naik *et al.*, *Bull. Am. Phys. Soc.* **43**, 416 (1998).
- ¹⁶For a comprehensive review of the diamond anvil cell and related optical techniques, see A. Jayaraman, *Rev. Mod. Phys.* **55**, 65 (1983), and the references therein.
- ¹⁷G. Burns and F. H. Dacol, *Phys. Rev. B* **18**, 5750 (1978).
- ¹⁸A. Pinczuk, W. T. Taylor, E. Burstein, and I. Lefkowitz, *Solid State Commun.* **5**, 429 (1967).
- ¹⁹L. Rimai, J. L. Parsons, J. T. Hickmott, and T. Nakamura, *Phys. Rev.* **168**, 623 (1968).
- ²⁰M. DiDomenico, Jr., S. H. Wemple, S. P. S. Porto, and R. P. Bauman, *Phys. Rev.* **174**, 522 (1968).
- ²¹G. Burns and B.A. Scott, *Solid State Commun.* **9**, 813 (1971).
- ²²L. H. Robins, D. L. Kauser, L. D. Rotter, and G. T. Stauff, in *Epitaxial Oxide Thin Films and Heterostructures*, edited by D. K. Fork *et al.*, MRS Symposia Proceedings No. 341 (Materials Research Society, Pittsburgh, 1994), p. 315.
- ²³The dip at 186 cm^{-1} has been observed in our samples when the Rayleigh tail at low frequencies was reduced considerably.
- ²⁴V. Lemos and F. Camargo, *J. Raman Spectrosc.* **21**, 123 (1990).
- ²⁵R. Comes and M. Lambert, *Solid State Commun.* **7**, 305 (1969).
- ²⁶Y. Akishage, J. Nakahara, and E. Sawaguchi, *J. Phys. Soc. Jpn.* **60**, 115 (1991).